Published in final edited form as:
Circ Res. 2006 June 23; 98(12): 1498–1505.

Selectivity of Cx43 channels is regulated through PKC-dependent phosphorylation

Jose F. Ek-Vitorin[1], **Timothy J. King**[2,†], **Nathanael S. Heyman**[1], **Paul D. Lampe**[2], and **Janis M. Burt**[1]

1 *Department of Physiology, University of Arizona*

2 *Division of Public Health Sciences, Fred Hutchinson Cancer Research Center*

Abstract

Coordinated contractile activation of the heart and resistance to ischemic injury depend, in part, on the intercellular communication mediated by Cx43-composed gap junctions. The function of these junctions is regulated at multiple levels (assembly to degradation) through phosphorylation at specific sites in the carboxyl terminus (CT) of the Cx43 protein. We show here that the selective permeability of Cx43 junctions is regulated through PKC-dependent phosphorylation at serine 368 (S368). Selective permeability was measured in several Cx43-expressing cell lines as the rate constant for intercellular dye diffusion relative to junctional conductance. The selective permeability of Cx43 junctions under control conditions was quite variable, as was the open state behavior of the comprising channels. Co-expression of the CT of Cx43 as a distinct protein, treatment with a PKC inhibitor, or mutation of S368 to alanine all reduced (or eliminated) phosphorylation at S368, reduced the incidence of 55–70pS channels, and reduced by ten fold the selective permeability of the junctions for a small cationic dye. Since PKC activation during pre-ischemic conditioning is cardio-protective during subsequent ischemic episodes, we examined no-flow, ischemic hearts for Cx43 phosphorylated at S368 (pS368). Consistent with early activation of PKC, pS368-Cx43 was increased in ischemic hearts; despite extensive lateralization of total Cx43, pS368-Cx43 remained predominantly at intercalated disks. Our data suggest that the selectivity of gap junction channels at intercalated disks is increased early in ischemia.

Keywords

gap junction; connexin 43; phosphorylation; selectivity; ischemia

Introduction

Gap junctions are clusters of intercellular channels that mediate electrical and chemical signaling throughout the cardiovascular system.[1;2] Gap junction channels are formed when hemichannels (connexons) in the membranes of neighboring cells dock. Each hemichannel is a hexamer of connexin subunits; in cells of the cardiovascular system four members of the connexin gene family are commonly expressed - Cx45, Cx43, Cx40, and Cx37. The predominant connexin expressed in ventricular cells is Cx43, the focus of the current study. In the normally functioning ventricle, Cx43 is localized to intercalated disks where it supports

†Present Address: Hawaii Biotech, Inc., 99-193 Aiea Heights Dr. Aiea, HI 96701

Janis M. Burt, Ph.D., Jose Ek Vitorin, M.D., Ph.D., Nathanael Heyman, Department of Physiology, PO Box 245051, Tucson, Arizona 85724, USA, Voice: (520) 626-6833, FAX: (520) 626-2383, jburt@u.arizona.edu ekvitori@u.arizona.edu nheyman@email.arizona.edu

Paul A. Lampe, Ph.D. Timothy, J. King, Ph.D.,Fred Hutchinson Cancer Research Center, Mail stop M5C800, 1100 Fairview Ave, Seattle, WA 98109, USA, Voice: (206) 667-4123 FAX: (206) 667-2537 plampe@fhcrc.org tking@hibiotech.com

the longitudinal and zigzag transverse spread of the action potential, such that coordinated contractile activation of the heart occurs. The contractile failure and arrhythmias occurring during ischemia reflect, in addition to compromised metabolism, altered excitability and reduced electrical coupling.[3]

Exposure of the heart to a brief period of ischemia and reperfusion (termed ischemic preconditioning) prior to a prolonged ischemic period protects the heart against necrosis and fatal arrhythmias.[4] During the ischemic preconditioning period receptor mediated activation of protein kinase C (PKC) occurs and appears to be necessary for protection against injury during the subsequent prolonged ischemic period. Thus, PKC activation (and translocation to the particulate fraction) is the initial step in a complex cascade of intracellular events that constitute an intrinsic defense strategy.[5] The immediate consequences of PKC activation are unclear but ultimately, during the subsequent prolonged ischemic period, apoptosis is reduced, the cytoskeleton stabilized, and mitochondrial function preserved. Some of these effects may well be mediated by kinases such as MAPK and Src, which are activated in parallel with or downstream from PKC activation.

PKC, MAPK and Src directly phosphorylate Cx43, effecting an acute (within minutes) reduction of channel conductance and/or open probability.[6–10] Over a somewhat longer time frame (tens of minutes to multiple hours) activation of these kinases leads to compromised Cx43 targeting/retention at intercalated disks and ultimately Cx43 gene expression.[11;12] In the heart, these phosphorylation-dependent changes in gap junction function likely contribute to an overall reduction in conduction velocity and increased dispersion of action potential duration and refractory properties, which combine to form the substrate for potentially lethal arrhythmias.[13] Consequently, these phosphorylation events appear to be counter-productive to continued coordinated activation of the heart and yet are ultimately protective to the heart and to other tissues in injury settings.[14–16] These apparently contradictory observations suggest that phosphorylation modulates an as yet unidentified parameter of channel function (e.g. selectivity) in a manner that is ultimately beneficial to tissue survival. We showed previously that S368 is required for a PKC-mediated reduction in channel conductance.[8] We show here that this site is involved in regulating the selective permeability of the junction. We further show that following 30 minutes of flow-deprivation at 37°C, Cx43 phosphorylated at this site was increased (despite ongoing gap junction remodeling) and remained predominantly localized at the intercalated disks.

Methods

Cells

Normal rat kidney epithelial (NRK) cells, transfected (or not) with the CT of Cx43 (NRK-CT)[17]; Rin43 cells, a rat insulinoma cell line stably transfected with rCx43 (CMV promoter)[18]; Re43 and Re43-S368A cells, derived from Cx43−/− cells stably transfected with rCx43 (22C-3 or MC:Re43)[19;20] or rCx43-S368A (pI8),[18] and Chinese Hamster Ovary (CHO) cells transfected with hOCT2, were all grown and maintained as appropriate (see *Online Methods*).

Junctional Permeability and Conductance, Single Channel Conductance

[21]Cells were visualized on an upright microscope equipped for epifluorescence and differential interference contrast (DIC) observation. The donor cell was accessed with a patch-type microelectrode containing our standard solution,[21;22] 0.1 mg/mL of rhodamine-labeled dextran (~3000Da) and either 0.25 mmol/L NBD-M-TMA (N,N,N-trimethyl-2-[methyl(7-nitro-2,1,3-benzoxadiazol-4-yl)amino]ethanamimium, charge 1+, MW 280 Da[23]) or 1 mmol/L LY (Lucifer Yellow CH, charge 2−, 443 Da,). Multiple images of NBD-M-TMA or LY

fluorescence were acquired;[21] after 10–20 minutes the recipient cell was accessed and both cells voltage clamped (0mV holding potential) to assess macroscopic (V_j=10mV) and single channel (V_j=40mV, following application of halothane) conductances using standard techniques but with discontinuous single electrode voltage clamp amplifiers.[21] Rhodamine-dextran fluorescence was typically imaged after measurements of junctional conductance. (See *Online Methods* for more details).

Data Analysis

Junctional permeability to a specific dye was quantified as the rate constant for intercellular diffusion of that dye (k_2) according to the procedures described by Ek-Vitorin & Burt[21]. The selective permeability for a specific dye was calculated as $k_{2\text{-dye}}/g_j$. Junctional conductance (g_j) and channel conductances were calculated from Ohm's law as customary (see *Online Methods*). Single channel conductances were binned in 5pS bins.

Whole heart studies

All mouse studies were conducted under Institutional Animal Care and Use Committee approval (FHCRC). Inbred mice (11 months of age in a FVB/N:C57BL6 background) were anaesthetized (avertin, 0.83mg/g body weight), hearts excised and placed either in cold PBS (with or without 1.8 mmol/L calcium, glucose free) for 30–60 seconds (control group) or incubated without coronary perfusion in warm (37°C), non-oxygenated PBS for 30 minutes ("ischemic group"). Although not thoroughly characterized,[24] this treatment reproduces the effects of ischemia on Cx43 electrophoretic mobility and gap junction remodeling (see results) demonstrated in better characterized models of ischemia.[25;26] Hearts in both groups were next longitudinally bisected and either immediately sonicated in Laemmli sample buffer (for Western analysis) or fixed overnight at 4°C in 10% formalin (for immunohistochemistry).

Western blots

(see *Online Methods*) After blotting, protein was detected with rabbit primary antibodies against pS368-Cx43 (1:1000, Cell Signaling, Inc), GAPDH (Ambion), or vinculin (Sigma) and mouse anti-Cx43NT.[27] Primary antibodies were visualized with either AlexaFluor 680 goat anti-rabbit (Molecular Probes) or IRDye800-conjugated donkey anti-mouse IgG (Rockland Immunochemicals), and directly quantified using the LI-COR Biosciences Odyssey infrared imaging system and associated software (inverted images are shown).

Immunohistochemistry

Formalin-fixed tissue was paraffin embedded, sectioned (4μm), immuno- and counter-stained (H&E), and microscopically analyzed as previously described.[28] (See *Online Methods*)

Results

Gap Junction Selective Permeability – control setting

The rate constant (k_2) for intercellular diffusion of either LY ($k_{2\text{-LY}}$) or NBD-M-TMA ($k_{2\text{-NBD}}$) was determined and related to the junction's conductance (g_j)[21] in NRK (endogenous expression of rCx43),[29;30] Rin43[31;32] and Re43[20] cells. Figure 1 illustrates our strategy for determining k_2. Panels A & B show DIC, LY or NBD fluorescence, and rhodamine-dextran fluorescence images of pairs of NRK cells. Fluorescence intensity as a function of time is plotted for both donor and recipient cells in panels C (LY) & D (NBD-M-TMA), and the recipient cell's fluorescence was fit to determine k_2 for each junction.[21] Although g_j was nearly two fold larger in the LY cell pair, the rate constant for intercellular diffusion of LY vs. NBD-M-TMA was nearly 10 fold less. $k_{2\text{-NBD}}$ vs. g_j data from 25 NRK pairs, 26 Rin43 pairs, 7 Re43 pairs, and $k_{2\text{-LY}}$ vs. g_j data for 10 NRK pairs (g_j>1nS for all pairs) are plotted in Figure 1E.

Neither $k_{2\text{-NBD}}$ or $k_{2\text{-LY}}$ was linearly related to g_j ($R2_{NBD}$=0.07; R^2_{LY}=0.133). On average $k_{2\text{-LY}}$ was nearly ten fold lower than $k_{2\text{-NBD}}$ (NBD-M-TMA: 1.07±0.20 sec^{-1}, n=25; LY: 0.13 ±0.04 sec^{-1}, n=10; p<0.0001).

NBD-M-TMA was designed as a fluorescent substrate for organic cationic transporters (e.g. OCT-1 & OCT-2),[23] and was later recognized as a superb junctional permeant. [21] To rule out a possible contribution of OCTs to the lack of linear relationship between k_2 and g_j, we cocultured Rin43 or NRK cells with hOCT2-transfected CHO cells, exposed the co-cultures to 250 μM NBD-M-TMA for 10 minutes under conditions that support OCT-mediated facilitated diffusion, and examined the cells for dye uptake. Neither the NRK or Rin43 cells expressed functional OCT-mediated uptake (Figure 2); however, when these cells formed contacts with the hOCT2-CHO cells they were sometimes observed to contain dye. These results indicate that OCT mediated transport played no role in the variable relationship between k_2 and g_j and further indicate that heterocellular junctions capable of supporting intercellular dye diffusion can form between OCT2-CHO and other Cx43 expressing cells.

Non-linearity of intercellular dye permeability vs. junctional conductance

If the selective permeability of all channels comprising Cx43 junctions were identical, then k_2 and g_j would be expected to increase in a related fashion as the number of junctional channels increased. A linear relationship between ostensibly comparable parameters was previously reported[33] for LY permeation of Cx43 junctions as formed by HeLa cells; thus the result shown in Figure 1E was unexpected. Because multiple open states are commonly observed in many Cx43-expressing cells but not in HeLa cells,[33–35] we hypothesized that the lack of linear correlation between k_2 and g_j observed in our experiments reflected differential phosphorylation of Cx43, one indicator of which is variable channel open state behavior.[8] To evaluate this possibility, we studied channel behavior;. figure 3 shows multiple segments of single channel records and associated all-points histograms derived from Rin43 (A–C) and NRK (D–F) cell pairs. Successive traces from the same cell pair as well as from different pairs demonstrated that not all channels in the junctions formed by these cells opened to the same conductance level. Figure 4 shows amplitude histograms compiled from multiple Rin43 (A) or NRK (B) cell pairs; for both cell types multiple open states were evident but their relative frequencies differed. Shown in Figure 4C (Rin43) & D (NRK) are amplitude histograms derived from cell pairs with high vs. low selective permeability for NBD-M-TMA ($k_{2\text{-NBD}}/g_j$). The data show that high selective permeability for NBD-M-TMA occurred in pairs with a high incidence of 55–70pS channels, whereas low selective permeability for NBD-M-TMA was observed in pairs where such events were rare.

pS368 and junctional selective permeability

We hypothesized that phosphorylation of Cx43 at S368 was necessary for high junctional NBD-M-TMA selective permeability. We used three strategies to reduce the contribution of pS368 to total Cx43 protein: the Rin43 cells were treated with the PKC inhibitor BIM (bisindolylmaleimide); the parental fibroblast line used to create the Re43 cells[8] was stably transfected with Cx43-S368A; and the NRK cells were transfected such that expression of the CT of Cx43 as a separate entity could be induced.[17] To demonstrate that over-expression of the CT was effective at reducing the contribution of pS368, we immunoblotted total protein from NRK and NRK-CT cells for total and pS368-Cx43 content. The NRK cells endogenously expressed Cx43 in P and P_0 forms (Figure 5). Induced expression of the CT did not significantly change total Cx43 expression; however, pS368-Cx43 content was decreased by 30% (p<0.015).

Figure 6 shows single channel records with all points histograms for BIM treated Rin43 (A,B) and NRK-CT (C,D) cells. In both groups, 55–70pS events like those in C were rarely observed.

Figure 7 shows amplitude histograms compiled from multiple pairs of BIM treated Rin43 (B) and NRK-CT (C) cells. The contribution of 55–70pS events to the total population of events was drastically reduced in both groups.

The $k_{2\text{-NBD}}$ vs. g_j plots for the three pS368-reduction strategies revealed that $k_{2\text{-NBD}}$ was significantly reduced (control: 0.83±0.12 min^{-1} (n=51); pS368-reduced: 0.20±0.05 min^{-1} (n=32), $p<0.0001$) particularly at lower g_j values (compare k_2 vs g_j plot in Figure 7A to that in 1E, graphed with comparable axis scaling). These data strongly suggest that phosphorylation at S368 is necessary for high selective permeability for NBD-M-TMA as well as the 55–70pS open state. The overall effect of such channels on selective permeability was evident in the significant reduction in $k_{2\text{-NBD}}/g_j$ resulting from BIM treatment of Rin43 cells ($k_{2\text{-NBD}}/g_j$ in Rin43: 0.12 ± 0.04 $min^{-1}nS^{-1}$, n=26 vs. Rin43+BIM: 0.02 ± 0.007 $min^{-1}nS^{-1}$, n=6; $p<0.02$) or CT expression in NRK cells ($k_{2\text{-NBD}}/g_j$ in NRK: 0.33±0.10 $min^{-1}nS^{-1}$, n=25 vs. NRK-CT: 0.05±0.02 $min^{-1}nS^{-1}$, n=13; $p<0.014$). Low $k_{2\text{-NBD}}/g_j$ values were also obtained for cells expressing the Cx43-S368A mutant (0.02 ± 0.009 $min^{-1}nS^{-1}$, n=8).

Phosphorylation of Cx43 in ischemic heart

The data presented above suggest that permeability and conductance are parameters of Cx43 channel function regulated by PKC-dependent phosphorylation of Cx43 at S368. PKC activation during ischemic preconditioning treatments is cardioprotective during subsequent ischemic events; consequently, we asked whether phosphorylation at this residue increased early during no-flow ischemia. Previous studies showed that the electrophoretic mobility of Cx43 isolated from ischemic heart is increased, such that most of the protein travels in a band that co-migrates with dephosphorylated Cx43, the P_0 band.[25] The P_0 band can, however, contain Cx43 phosphorylated at S368.[29] Consequently, we evaluated total protein isolated from three control and three ischemic hearts for total Cx43 and pS368-Cx43. Consistent with previous observations the electrophoretic mobility of Cx43 isolated from our no-flow ischemic hearts was increased compared to normal (Figure 8A, each lane represents a separate heart). In addition, a decrease of total Cx43, possibly due to some loss of the protein during ischemia or, alternatively, to lower avidity of the antibody for less phosphorylated forms of Cx43, was observed. Figure 8A further shows that pS368-Cx43 content increased ~5 fold ($p<0.02$) relative to total Cx43 in the ischemic hearts, and that nearly all of this pS368-Cx43 co-migrated with the “dephosphorylated” Cx43 (P_0 band). Identical results were obtained whether the PBS contained 1.8 mmol/L $CaCl_2$ or was calcium-free; moreover, the described changes in electrophoretic mobility of Cx43 were evident, though less prominently, after only 5 minutes of no-flow ischemia (not shown).

The distribution of pS368-Cx43 vs. total Cx43 in ischemic vs. control tissue was quite distinct. Figure 8B shows that in control hearts virtually all Cx43 was localized to intercalated disks. As shown previously for the ischemic heart,[25] a considerable increase in Cx43 localized at the lateral borders of myocytes was observed in the ischemic group hearts. Cx43 phosphorylated at S368 was largely absent in control hearts but significantly increased in the ischemic group hearts; despite obvious gap junction remodeling most of the pS368-Cx43 remained localized at intercalated disks in these hearts.

Discussion

Selective permeability, phosphorylation and ion flux

Receptor mediated PKC activation occurs in most tissues in response to growth and injury stimuli - settings where functional gap junctions are crucial to normal tissue response.[1;4] In Cx43 expressing cells, including ventricular myocytes, PKC activation results in reduced dye coupling (LY, 6-carboxyfluorescein), which could reflect the combined effects of reduced

channel number, open probability or permeability.[6;11;36;37] Using quantitative methods we show here that permeation of Cx43 gap junctions by NBD-M-TMA varies widely and without a linear correlation with their own g_j values under control conditions. This variability was reduced nearly ten fold (to a level comparable to LY) when phosphorylation at S368 was reduced, blocked or eliminated. The data indicate that the selectivity of Cx43 gap junction channels is regulated via phosphorylation-dependent mechanisms, and suggest that phosphorylation at S368 leads to reduced permeation by current carrying ions (predominantly K and Cl) but enhanced permeation by some larger molecules (e.g. NBD-M-TMA).

Successful permeation of gap junction channels depends on the size, charge, shape and molecular constituents of candidate permeants.[38] Connexin-specific selectivity differences can be as large as 300 fold,[27;39] and discrimination between extremely similar solutes by any homotypic channel can be profound.[40] Nevertheless, Valiunas et al[33] concluded from Cx43-expressing HeLa cells studied with LY that junctional permeability and conductance were linearly related, a result strikingly different from that reported here and elsewhere.[21;41;42] It is tempting to suggest that the differing results could reflect differences in methodology, sample size, cell-specific regulation of Cx43 and/or dye selection. The fully open state of Cx43 is heavily favored in HeLa cells (long-lived substate behavior is infrequent), suggesting that the impact of phosphorylation on channel permeability and substate behavior is low. Further, the PKC-induced channel conformation(s) may not be as readily permeated by Lucifer Yellow as NBD-M-TMA (as the data herein suggest), in which case its presence would be poorly detected with LY. Thus, the conditions of the Valiunas study[33] may not have been favorable for observation of variable permeability.

Previously reported estimates of per channel flux rates for Cx43 differed by 400 fold: ~750 molecules/s for LY[33] vs. ~300,000 molecules/s for Alexa488,[38] a range comparable to that recently reported by Eckert.[42] Although the methodology used in these studies differed, two method-independent explanations were advanced to explain the differing per channel flux rates. First, permeant-pore interactions were suggested to limit the diffusion of LY through the pore to a far greater extent than Alexa 488 (despite their similar size and charge); second, the permeation state of the Cx43 channels formed in oocytes[38] vs. HeLa[33] cells differed, possibly due to cell-specific differential phosphorylation. The range of per channel flux rates for NBD-M-TMA (calculated from k_2 and junctional conductance, assuming a cell volume of 1pL, dye concentration of 1 mmol/L, and channel conductance of 105pS) observed under control conditions in our study was 6,600 to 2,000,000 molecules/sec, an ~300 fold difference for the same permeant. Treatments aimed at decreasing or eliminating pS368 reduced the range (as much as 80 fold) and mean (as much as 7 fold) observed $k_{2\text{-NBD}}$ (see *Online Supplemental Data*), but notably, none of the pS368 reduction strategies resulted in a uniform population of fully open (100–120pS) channels and none resulted in a linear $k_{2\text{-NBD}}$ vs. g_j relationship. Thus, our results indicate that, indeed, selective permeability is a regulated parameter of junctional function that involves changes in the relative contribution to the junction of channels with high vs. intermediate or low selectivity and is, in part, determined by phosphorylation of the channel proteins at S368.

Despite the wide variability and sometimes very high $k_{2\text{-NBD}}$ and $k_{2\text{-NBD}}/g_j$ values, the per channel flux rate for dye was always less than that for K^+, basically because the mobility of K + in solution is ~10 fold greater than that of the dye. For a sensible estimation of NBD-M-TMA:K flux ratio, a comparison of flux due to a concentration gradient (according to Fick's law) vs. an electrical gradient (according to Ohms Law) was done (see *Online Supplemental Data*). The results show that NBD-M-TMA:K flux was 1:4.5 (0.22) for channels in junctions with the highest selective NBD-M-TMA permeability; however, for most channels the NBD-M-TMA:K flux ratio of 0.011 was comparable to that reported for LY:K (0.025).[33]

Our data suggest that phosphorylation of the Cx43 at S368 increases the permeability of the channel by as much as 300 fold yet either has no effect on or reduces the conductance of the channel by only 2 fold. One model of channel function that accommodates a stable or decreased conductance but increased large molecule permeation involves phosphorylation-induced stabilization of the fluid movements of the CT such that random interference with pore entry by large molecules is reduced (permeation increased). Testing this model (and others) will clearly require additional work, but it represents a plausible starting point for such investigations.

Physiological relevance of junctional selectivity

The possible significance of regulated selectivity is suggested by our data showing a significant increase in pS368-Cx43 early during no-flow ischemia as well as by its timely appearance in wound healing.[43] The latter study showed that pS368-Cx43 was uniformly distributed in unwounded human epidermal layers; however, at 24 but not 6h post-wounding pS368-Cx43 levels were substantially increased in basal keratinocytes and virtually eliminated from the suprabasal layers in the region of the wound. These alterations in Cx43 phosphorylation and localization were suggested to result in the formation of communication compartments in the region of the wound that might facilitate repair and delay differentiation in suprabasal cells until appropriate.

Relative to the heart, the data presented herein indicate that early in no-flow ischemia phosphorylation of Cx43 at S368 increases significantly, despite dephosphorylation and relocation of substantial amounts of Cx43 to lateral borders. Given the enhanced permselectivity of Cx43 channels and junctions containing pS368-Cx43, the localization of pS368-Cx43 to intercalated disks suggests that intercellular signaling along the longitudinal vs. transverse axes might differ in the ischemic vs. normal heart. Reduced longitudinal conduction velocity is expected (and observed) consequent to the reduction at intercalated disks of channel number and conductance (due to pS368). Transverse conduction is not, however, expected to increase in parallel with the redistribution of Cx43 to the lateral borders, as dephosphorylated Cx43 does not assemble channels efficiently.[30;44] Due to the complexity of impulse propagation in the heart, it is not entirely clear that these (combined) effects of Cx43 phosphorylation/dephosphorylation and relocation are antiarrhythmic; however, PKC activation occurs during ischemic preconditioning, is required for the protection (against arrhythmias and cell injury) conferred by preconditioning, and is sufficient to protect the ischemic heart against ischemic injury.[45–47] We therefore suggest that in addition to any electrical benefits that phosphorylation at S368 might confer on the ischemic heart, the metabolic and signaling consequences of altered selective permeability on tissue survival and repair might be more profound.[43] For instance, by facilitating or preventing the intercellular movement (between non-ischemic and ischemic cells) of metabolites and signaling molecules, altered junctional selective permeability might be crucial for cell survival and tissue function during and following ischemic insults.

Supplementary Material

Refer to Web version on PubMed Central for supplementary material.

Acknowledgements

These studies were supported by Grants from the National Institutes of Health: HL058732, HL076260-02 (JMB), GM055632 (PDL), and the American Heart Association, Pacific Mountain Affiliate (JMB), #0550258z.

References

1. Saez JC, Berthoud VM, Branes MC, Martinez AD, Beyer EC. Plasma membrane channels formed by connexins: their regulation and functions. Physiol Rev 2003;83:1359–1400. [PubMed: 14506308]
2. Severs NJ, Coppen SR, Dupont E, Yeh HI, Ko YS, Matsushita T. Gap junction alterations in human cardiac disease. Cardiovasc Res 2004;62:368–377. [PubMed: 15094356]
3. Severs NJ, Dupont E, Coppen SR, Halliday D, Inett E, Baylis D, Rothery S. Remodelling of gap junctions and connexin expression in heart disease. Biochim Biophys Acta 2004;1662:138–148. [PubMed: 15033584]
4. Cohen MV, Baines CP, Downey JM. Ischemic preconditioning: from adenosine receptor to KATP channel. Annu Rev Physiol 2000;62:79–109. 79–109. [PubMed: 10845085]
5. Dawn B, Bolli R. Role of nitric oxide in myocardial preconditioning. Ann NY Acad Sci 2002;962:18–41. [PubMed: 12076960]
6. Moreno AP, Saez JC, Fishman GI, Spray DC. Human Connexin43 gap junction channels: regulation of unitary conductances by phosphorylation. Circ Res 1994;74:1050–1057. [PubMed: 7514508]
7. Cottrell GT, Lin R, Warn-Cramer BJ, Lau AF, Burt JM. Mechanism of v-Src- and mitogen-activated protein kinase-induced reduction of gap junction communication. Am J Physiol Cell Physiol 2003;284:C511–C520. [PubMed: 12388103]
8. Lampe PD, Tenbroek EM, Burt JM, Kurata WE, Johnson RG, Lau AF. Phosphorylation of connexin43 on serine368 by protein kinase C regulates gap junctional communication. J Cell Biol 2000;149:1503–1512. [PubMed: 10871288]
9. Warn-Cramer BJ, Cottrell GT, Burt JM, Lau AF. Regulation of connexin43 gap junctional intercellular communication by mitogen-activated protein kinase. J Biol Chem 1998;273:9188–9196. [PubMed: 9535909]
10. Cameron SJ, Malik S, Akaike M, Lee JD, Lerner-Marmarosh N, Yan C, Abe JI, Yang J. Regulation of EGF-induced Connexin 43 gap junction communication by BMK1/ERK5 but not ERK1/2 kinase activation. J Biol Chem 2003;278:18682–18688. [PubMed: 12637502]
11. Laird DW. Connexin phosphorylation as a regulatory event linked to gap junction internalization and degradation. Biochim Biophys Acta 2005;1711:172–182. [PubMed: 15955302]
12. Solan JL, Lampe PD. Connexin phosphorylation as a regulatory event linked to gap junction channel assembly. Biochim Biophys Acta 2005;1711:154–163. [PubMed: 15955300]
13. Poelzing S, Rosenbaum DS. Nature, significance, and mechanisms of electrical heterogeneities in ventricle. Anat Rec A Discov Mol Cell Evol Biol 2004;280:1010–1017. [PubMed: 15368342]
14. Daleau P, Boudriau S, Michaud M, Jolicoeur C, Kingma JG Jr. Preconditioning in the absence or presence of sustained ischemia modulates myocardial Cx43 protein levels and gap junction distribution. Can J Physiol Pharmacol 2001;79:371–378. [PubMed: 11405239]
15. Qiu C, Coutinho P, Frank S, Franke S, Law LY, Martin P, Green CR, Becker DL. Targeting connexin43 expression accelerates the rate of wound repair. Curr Biol 2003;13:1697–1703. [PubMed: 14521835]
16. Coutinho P, Qiu C, Frank S, Wang CM, Brown T, Green CR, Becker DL. Limiting burn extension by transient inhibition of Connexin43 expression at the site of injury. Br J Plast Surg 2005;58:658–667. [PubMed: 15927148]
17. Shin JL, Solan JL, Lampe PD. The regulatory role of the C-terminal domain of connexin43. Cell Commun Adhes 2001;8:271–275. [PubMed: 12064601]
18. Vozzi C, Ullrich S, Charollais A, Philippe J, Orci L, Meda P. Adequate connexin-mediated coupling is required for proper insulin production. J Cell Biol 1995;131:1561–1572. [PubMed: 8522612]
19. Martyn KD, Kurata WE, Warn-Cramer BJ, Burt JM, Tenbroek E, Lau AF. Immortalized connexin43 knockout cell lines display a subset of biological properties associated with the transformed phenotype. Cell Growth Differ 1997;8:1015–1027. [PubMed: 9300183]
20. Hirschi KK, Burt JM, Hirschi KD, Dai C. Gap junction communication mediates transforming growth factor-beta activation and endothelial-induced mural cell differentiation. Circ Res 2003;93:429–437. [PubMed: 12919949]
21. Ek-Vitorin JF, Burt JM. Quantification of Gap Junction Selectivity. Am J Physiol Cell Physiol 2005;289:C1535–C1546. [PubMed: 16093281]

22. Cottrell GT, Wu Y, Burt JM. Functional characteristics of heteromeric Cx40-Cx43 gap junction channel formation. Cell Commun Adhes 2001;8:193–197. [PubMed: 12064587]
23. Bednarczyk D, Mash EA, Aavula BR, Wright SH. NBD-TMA: a novel fluorescent substrate of the peritubular organic cation transporter of renal proximal tubules. Pflugers Arch 2000;440:184–192. [PubMed: 10864014]
24. Sutherland FJ, Hearse DJ. The isolated blood and perfusion fluid perfused heart. Pharmacol Res 2000;41:613–627. [PubMed: 10816330]
25. Beardslee MA, Lerner DL, Tadros PN, Laing JG, Beyer EC, Yamada KA, Kleber AG, Schuessler RB, Saffitz JE. Dephosphorylation and intracellular redistribution of ventricular connexin43 during electrical uncoupling induced by ischemia. Circ Res 2000;87:656–662. [PubMed: 11029400]
26. Wit AL. Remodeling of cardiac gap junctions: the relationship to the genesis of ventricular tachycardia. J Electrocardiol 2001;34 (Suppl):77–83. [PubMed: 11781940]
27. Goldberg GS, Moreno AP, Lampe PD. Gap junctions between cells expressing connexin 43 or 32 show inverse permselectivity to adenosine and ATP. J Biol Chem 2002;277:36725–36730. [PubMed: 12119284]
28. King TJ, Lampe PD. The gap junction protein connexin32 is a mouse lung tumor suppressor. Cancer Res 2004;64:7191–7196. [PubMed: 15492231]
29. Solan JL, Fry MD, Tenbroek EM, Lampe PD. Connexin43 phosphorylation at S368 is acute during S and G2/M and in response to protein kinase C activation. J Cell Sci 2003;116:2203–2211. [PubMed: 12697837]
30. Cooper CD, Lampe PD. Casein kinase 1 regulates connexin-43 gap junction assembly. J Biol Chem 2002;277:44962–44968. [PubMed: 12270943]
31. Banach K, Weingart R. Connexin43 gap junctions exhibit asymmetrical gating properties. Pflugers Arch 1996;431:775–785. [PubMed: 8596730]
32. Cottrell GT, Burt JM. Heterotypic gap junction channel formation between heteromeric and homomeric Cx40 and Cx43 connexons. Am J Physiol Cell Physiol 2001;281:C1559–C1567. [PubMed: 11600419]
33. Valiunas V, Beyer EC, Brink PR. Cardiac gap junction channels show quantitative differences in selectivity. Circ Res 2002;91:104–111. [PubMed: 12142342]
34. Martinez AD, Hayrapetyan V, Moreno AP, Beyer EC. Connexin43 and connexin45 form heteromeric gap junction channels in which individual components determine permeability and regulation. Circ Res 2002;90:1100–1107. [PubMed: 12039800]
35. Bukauskas FF, Bukauskiene A, Verselis VK. Conductance and permeability of the residual state of connexin43 gap junction channels. J Gen Physiol 2002;119:171–186. [PubMed: 11815667]
36. Kwak BR, Jongsma HJ. Regulation of cardiac gap junction channel permeability and conductance by several phosphorylating conditions. Molecular and Cellular Biochemistry 1996;157:93–99. [PubMed: 8739233]
37. Doble BW, Chen Y, Bosc DG, Litchfield DW, Kardami E. Fibroblast growth factor-2 decreases metabolic coupling and stimulates phosphorylation as well as masking of connexin43 epitopes in cardiac myocytes. Circ Res 1996;79:647–658. [PubMed: 8831488]
38. Weber PA, Chang HC, Spaeth KE, Nitsche JM, Nicholson BJ. The permeability of gap junction channels to probes of different size is dependent on connexin composition and permeant-pore affinities. Biophys J 2004;87:958–973. [PubMed: 15298902]
39. Goldberg GS, Lampe PD, Nicholson BJ. Selective transfer of endogenous metabolites through gap junctions composed of different connexins. Nat Cell Biol 1999;1:457–459. [PubMed: 10559992]
40. Bevans CG, Kordel M, Rhee SK, Harris AL. Isoform composition of connexin channels determines selectivity among second messengers and uncharged molecules. J Biol Chem 1998;273:2808–2816. [PubMed: 9446589]
41. Biegon RP, Atkinson MM, Liu TF, Kam EY, Sheridan JD. Permeance of novikoff hepatoma gap junctions: quantitative video analysis of dye transfer. J Membr Biol 1987;96:225–233. [PubMed: 3612766]
42. Eckert R. Gap-junctional single channel permeability for fluorescent tracers in mammalian cell cultures. Biophys J. 2006in press

43. Richards TS, Dunn CA, Carter WG, Usui ML, Olerud JE, Lampe PD. Protein kinase C spatially and temporally regulates gap junctional communication during human wound repair via phosphorylation of connexin43 on serine368. J Cell Biol 2004;167:555–562. [PubMed: 15534005]

44. Musil LS, Goodenough DA. Biochemical analysis of connexin43 intracellular transport, phosphorylation, and assembly into gap junctional plaques. J Cell Biol 1991;115(5):1357–1374. [PubMed: 1659577]

45. Garcia-Dorado D, Ruiz-Meana M, Padilla F, Rodriguez-Sinovas A, Mirabet M. Gap junction-mediated intercellular communication in ischemic preconditioning. Cardiovasc Res 2002;55:456–465. [PubMed: 12160942]

46. Armstrong SC. Protein kinase activation and myocardial ischemia/reperfusion injury. Cardiovasc Res 2004;61:427–436. [PubMed: 14962474]

47. Cross HR, Murphy E, Bolli R, Ping P, Steenbergen C. Expression of activated PKC epsilon (PKC epsilon) protects the ischemic heart, without attenuating ischemic H(+) production. J Mol Cell Cardiol 2002;34:361–367. [PubMed: 11945027]

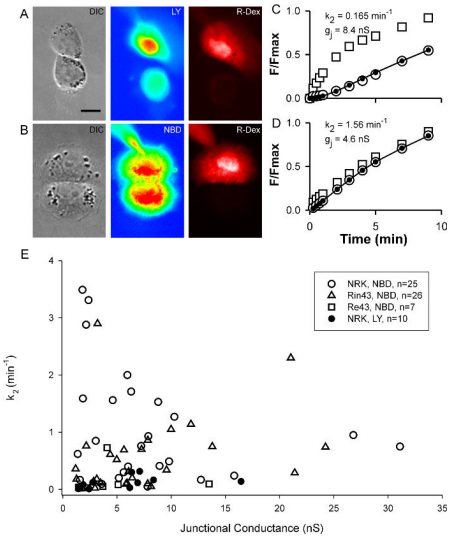

Figure 1.

Intercellular diffusion rate for LY and NBD-M-TMA in Cx43 expressing cells is not predicted by junctional conductance. A,B: DIC and false-colored fluorescence images of NRK cell-pairs showing LY (A) or NBD-M-TMA (B) in donor and recipient cells 5 minutes after access to the donor cell was achieved. For both cell pairs, rhodamine-dextran (R-Dex) was observed only in the donor cell, which indicates that a gap junction rather than a cytoplasmic bridge connected the cells (calibration 10μm). Panels C & D show, for the cells in A & B respectively, the time course of fluorescence increase (F/Fmax, where F is the fluorescence at the indicated time and Fmax the maximum observed fluorescence) in the donor (squares) vs. recipient cells (open circles). Closed circles and line represent the best-fit[21] of the recipient fluorescence data; k_2 and g_j values for each pair are noted in the figure. Panel E shows the k_2 vs. g_j values for multiple cell pairs - note the absence of correlation between the two parameters. The range of values for $k_{2\text{-NBD}}/g_j$ was considerably larger in NRK vs. Rin43 cells, 0.006 - 1.93 $\text{min}^{-1}\text{nS}^{-1}$ vs. 0.006 – 0.906 $\text{min}^{-1}\text{nS}^{-1}$, respectively.

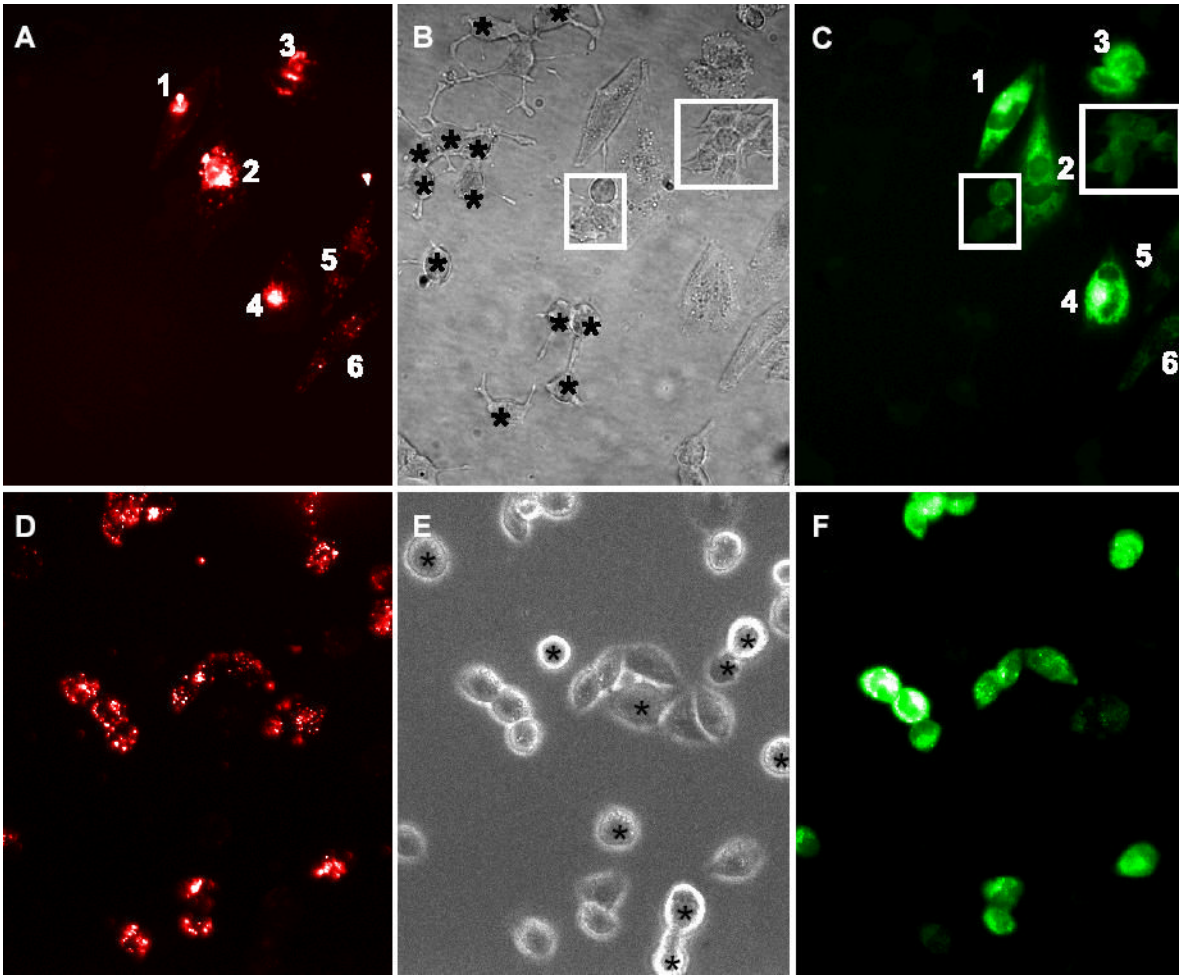

Figure 2.

NRK cells do not express functional organic cation transport. OCT expressing CHO cells prelabeled with DiI (red cells – left panel) were co-cultured with unlabeled NRK cells and exposed to 250wM NBD -M-TMA in Waymouth's buffer for ten minutes. NBD-M-TMA (green - right panel) cannot be detected in any NRK cells (labeled with asterisks in the phase image – center panel) despite robust uptake by the OCT expressing CHO cells. (Images presented in false color.)

Rin43 cells do not express functional organic cation transport. OCT expressing CHO cells prelabeled with DiI (red cells – left panel) were co-cultured with unlabeled Rin43 cells and exposed to 250wM NBD -M-TMA in Waymouth's buffer for ten minutes. Despite robust uptake of NBD-M-TMA (green - right panel) by the OCT expressing, dye is not detected in isolated Rin43 cells (labeled with asterisks in the phase image – center panel). Rin43 cells contacting a CHO cell either directly or via another Rin43 cell (boxed cells) receive dye in a contact dependent mechanism – gap junctions.

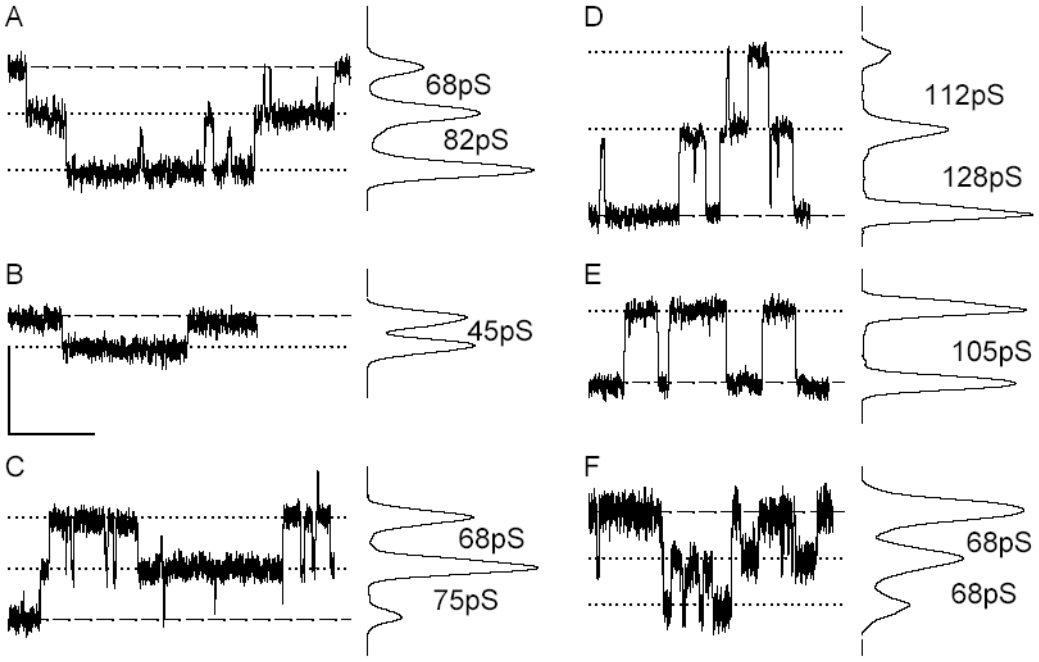

Figure 3.

Cx43 opens to multiple conductance levels in both Rin43 (A–C) and NRK (D–F) cells. Shown are single channel events and corresponding all points histograms obtained from the same pair of Rin43 cells (A,B) following two different halothane treatments and from a second pair of Rin43 cells (C). Similar data are shown for a pair of NRK cells (D,E) and a second NRK pair (F). Events of different amplitudes are evident both within and between pairs; conductances of corresponding channel events are indicated as inter-peak values on the all points histograms. Dashed lines indicate the position of zero current; dotted lines mark open state current levels. (V_j in all records: 40mV; calibrations: y=5pA, x=2s except for C where it is 4s; all records were sampled at 2kHz and subsequently filtered at 100Hz.)

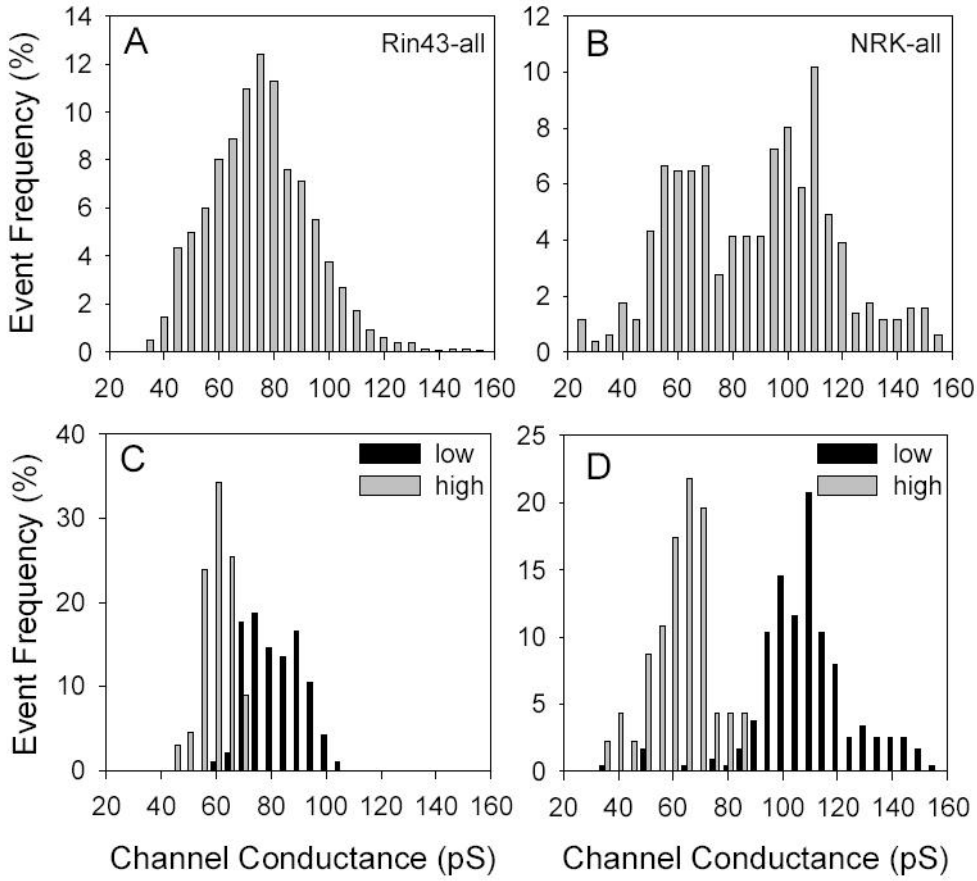

Figure 4.

Amplitude histograms reveal variable open state behavior of Cx43 channel in both Rin43 and NRK cells; high selective permeability for NBD-M-TMA occurred in pairs with a high incidence of 55-70pS events. A&B: Amplitude histograms compiled from multiple Rin43 (N=10, n=1384) and NRK pairs (N=5, n=511). C–D: Amplitude histograms derived from Rin43 or NRK cell-pairs with high vs. low NBD-M-TMA selective permeability. Selective permeability (in $min^{-1}nS^{-1}$): Rin43-low 0.013; Rin43-high 0.91; NRK-low 0.006; NRK-high 0.34. Total events: Rin43-low 96, Rin43-high 67, NRK-low 241, NRK-high 46. Note that 55-70pS events were rare in pairs with low junctional NBD-M-TMA selective permeability.

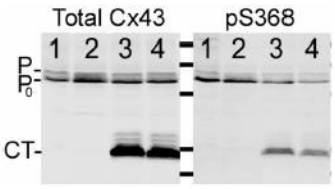

Figure 5.

Phosphorylation of Cx43 at S368 is reduced in NRK cells that express the CT of Cx43 as a separate protein. Total protein isolated from NRK (lanes 1 and 2) and NRK-CT cells (lanes 3 and 4) was probed for total Cx43 or pS368-Cx43. Note the 30% decrease in pS368-Cx43 relative to total Cx43 in the CT expressing NRK cells.

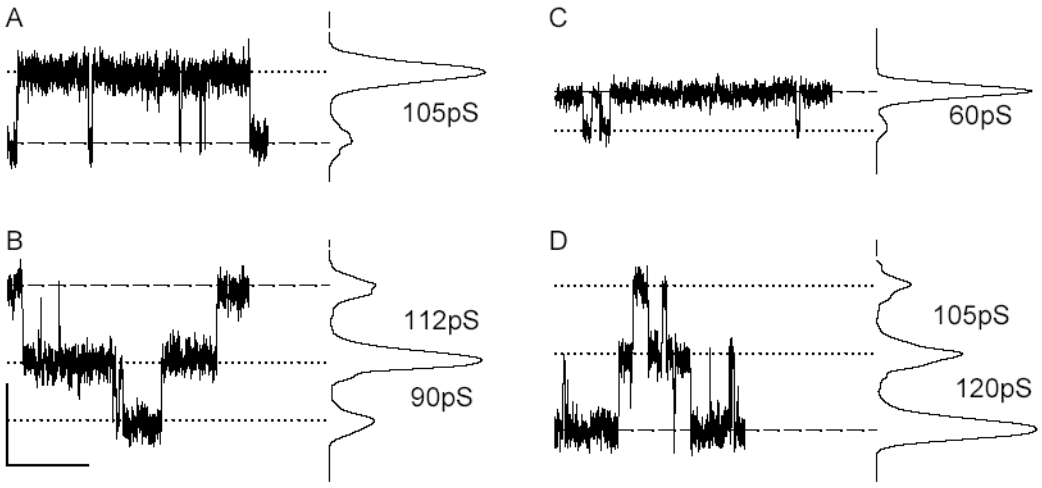

Figure 6.

Multiple open states are observed in Rin43 and NRK cells following treatments that reduced the contribution of pS368 to the total Cx43 protein pool. Shown are single channel events and corresponding all points histograms derived from BIM treated Rin43 cells (A,B) and NRK-CT cells (C,D). Events of different amplitudes are evident in both, although conductance states (indicated as inter-peak values on the all points histograms) smaller than the fully open 100-120pS) channel were rare in BIM treated Rin43 cells. Dashed line indicates the position of zero current; dotted lines mark open state current levels. (V_j in all records: 40mV; calibrations: y=5pA, x=2s; all records were sampled at 2kHz and subsequently filtered at 100Hz.)

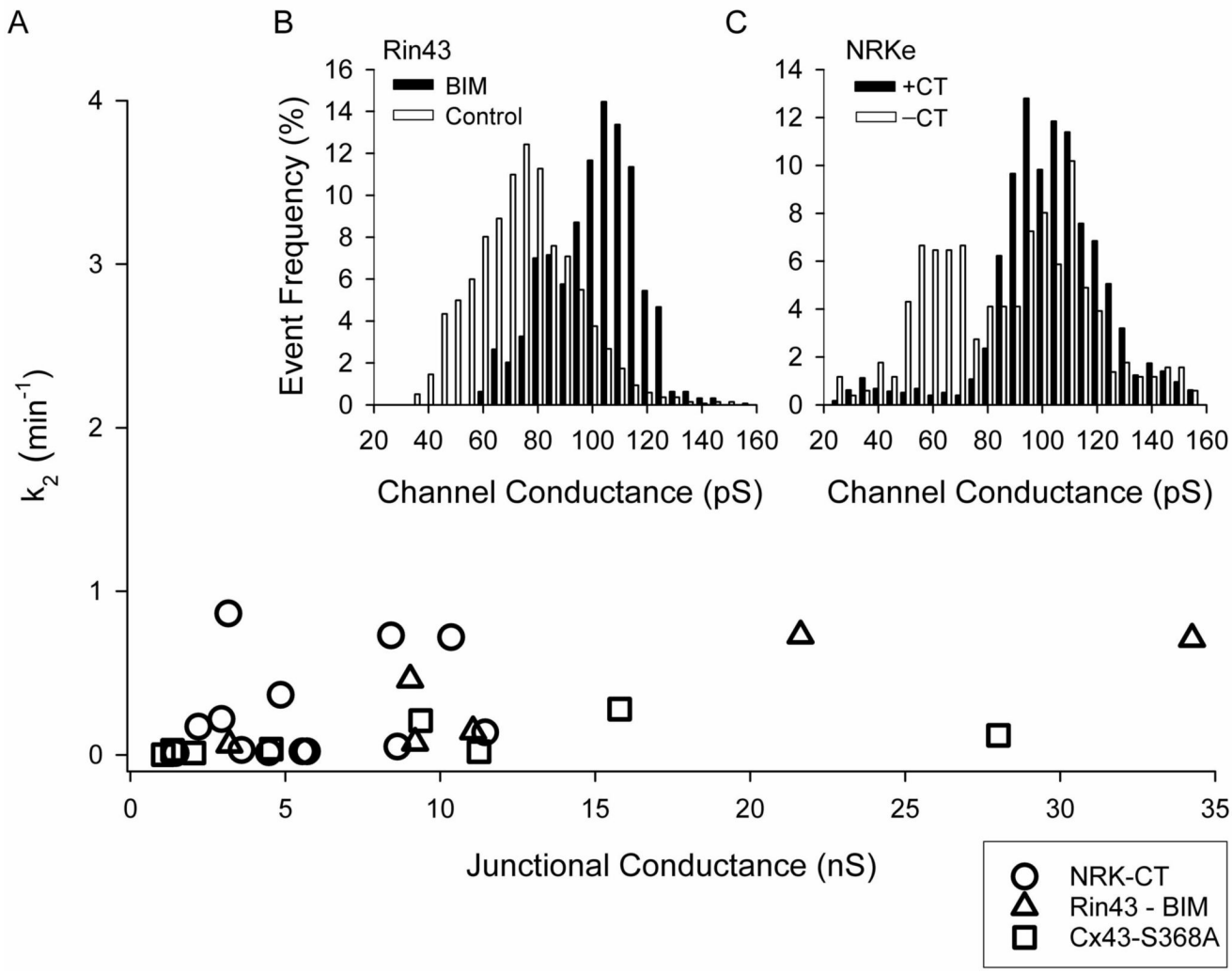

Figure 7.

Reduced pS368 levels lead to a decreased frequency of the 55-70pS open state and lowered junctional NBD-M-TMA selective permeability. In panel A $k_{2\text{-NBD}}$ as a function of g_j is plotted for NRK-CT (n=13), BIM treated Rin43 cells (n=6), and Re43-S368A (n=8). Junctions with high $k_{2\text{-NBD}}$ values were absent irrespective of junctional conductance (compare to figure 1E, which is plotted with the same x/y axis scaling). Panels B (Rin43-BIM, N=5, n=643) and C (NRK-CT, N=6, n=1786) show single channel conductance histograms obtained from the cell pairs illustrated in A for which single channel data were obtained (control data from figure 3 is shown for comparison). Note the significant reduction in frequency of the 55-70pS events.

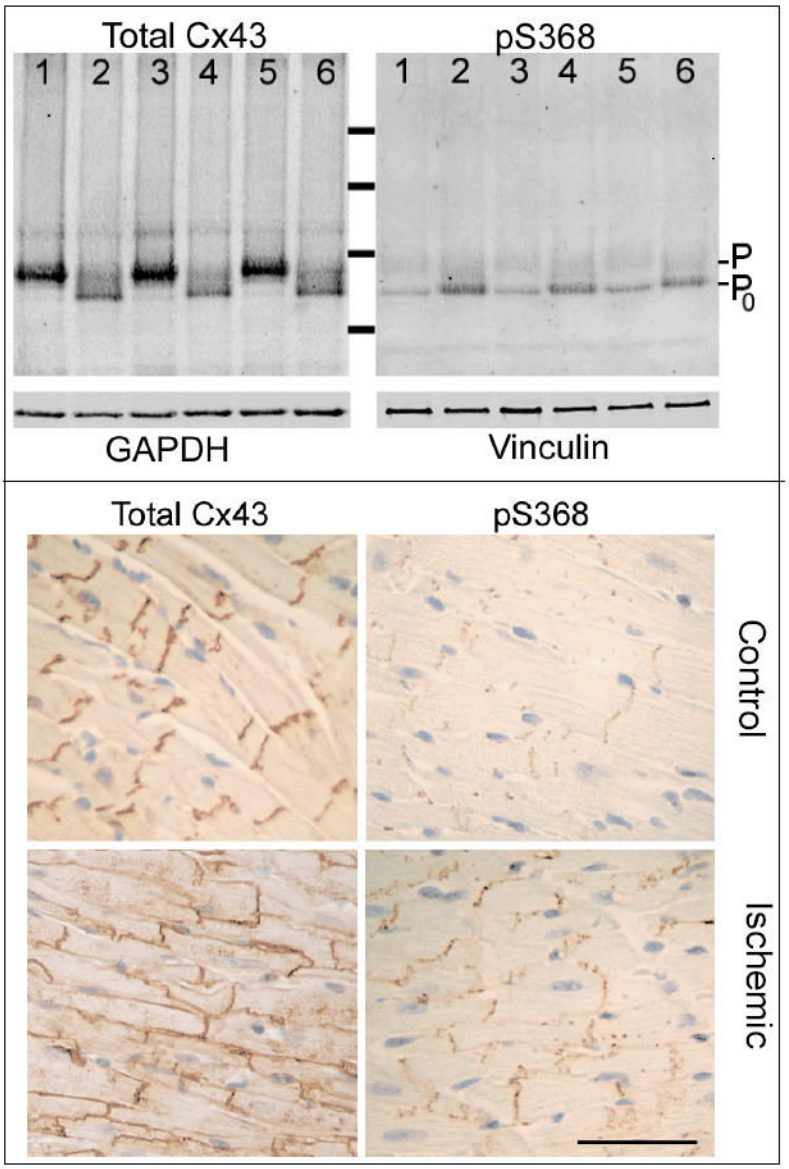

Figure 8.

Despite increased electrophoretic mobility of Cx43 isolated from ischemic vs. control hearts, phosphorylation at serine 368 was increased in ischemic heart. Western blots of total protein isolated from 3 control (Lanes 1,3,5) and 3 no-flow ischemic (30 minutes at 37°C; Lanes 2,4,6) hearts (each lane a distinct heart) probed for total Cx43 (N-terminal antibody) or pS368-Cx43. The total protein load per lane was approximately equal as shown by blotting an equally loaded gel with GAPDH and Vinculin antibodies (lower panels as marked). Note Cx43 phosphorylated at S368 increased ~5 fold in ischemic vs. control hearts.Cx43 distribution and phosphorylation are altered in ischemic vs. control hearts. In control tissue, Cx43 was localized to intercalated disks whereas in ischemic tissue Cx43 was fairly uniformly distributed around each myocyte. Cx43 phosphorylated at S368 was detected at low levels in control tissue but at high levels in ischemic tissue. Most of the pS368-Cx43 was localized to the intercalated disks, even in ischemic tissue. (Calibration 100μm).